1

Low Reynolds Number Flows and Transition

M. Serdar Genç[1], İlyas Karasu[1,2], H. Hakan Açıkel[1]
and M. Tuğrul Akpolat[1]
[1]*Wind Engineering and Aerodynamics Research Laboratory, Department of Energy Systems Engineering, Erciyes University, 38039, Kayseri*
[2]*İskenderun Civil Aviation School, Mustafa Kemal University, 31200, Hatay Turkey*

1. Introduction

Due to the advances in unmanned aerial vehicles (UAV), micro air vehicles (MAV) and wind turbines, aerodynamics researches concentrated on low Reynolds number aerodynamics, transition and laminar separation bubble (LSB) and its effects on aerodynamic performance. In order to improve endurance, range, efficiency and payload capacity of UAVs, MAVs and wind turbines, the aerodynamic behaviors of these vehicles mentioned should be investigated.

The range of Re numbers of natural and man-made flyers is shown in Figure 1. As the Figure 1 shows most of the commercial and military aircrafts operate on high Reynolds (Re) numbers, and the flow on the surface of these aircraft's wing doesn't separate until the aircraft reaches higher angles of attack -as the angle of attack increases the effects of adverse pressure gradients increase- due to having higher forces of inertia (Genç, 2009). The LSB can be encountered on flyers whose Re number is in the range of 10^4 to 10^6 (King, 2001). On low Re number flow regimes the effects of viscous forces are dominant, which may cause the laminar flow to separate. Under certain circumstances the separated flow which occurs by reason of an adverse pressure gradient reattaches and this forms the LSB. The LSB can be classified as short and long (Tani, 1964). Both short and long bubbles have negative effects on aerodynamic performance. These negative effects may increase drag and decrease lift owing to the altered pressure distribution caused by the presence of the LSB. The characteristics of the LSB depend on the airfoil shape, Re number, surface roughness, freestream disturbances (such as acoustic disturbances), freestream turbulence and geometric discontinuities.

In order to improve the aerodynamic performance, there are new methods being developed to eliminate the effects of the LSB, besides the high lift devices. These methods are called flow control methods and could be classified as active and passive. By using the flow control methods, drag force may be reduced, lift may be increased, stall may be delayed, noise and vibrations may be reduced and reattachment of the separated flow may be obtained.

The effects of the LSB and flow control methods on low Re flow has been investigated by means of various experimental methods, such as force measurement, velocity measurement by using hot-wire anemometry and particle image velocimetry (PIV), pressure measurement with pressure transducers, flow visualization with smoke wire, oil, InfraRed thermography, etc. These systems are useful and accurate but also expensive and everyone cannot find the opportunity to use these methods. Therefore investigating all kind of aerodynamic

phenomena via Computational Fluid Dynamics (CFD) is now popular and easier to use. By using CFD, the flow characteristics of a wing profile or the device (UAV, MAV, wind turbine) can be easily analyzed.

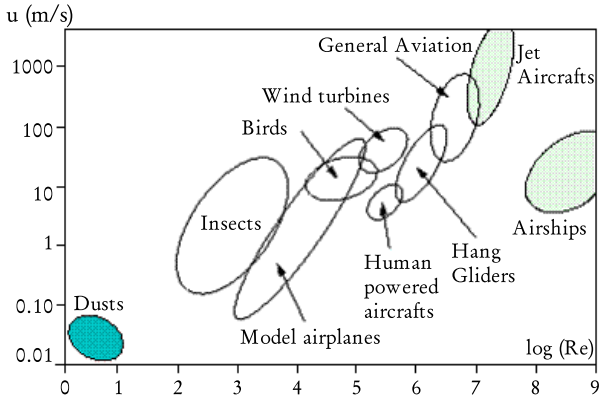

Fig. 1. Flight speeds versus Re number of aircrafts (Chklovski, 2012)

Low Re number flows are seen on mini, micro and unmanned air vehicles, wind turbine blades, model aircrafts, birds and little creatures like bees or flies. Under such low Reynolds numbers, the maximum lift and stall angle are lower than high Re number flow conditions. Owing to the fact that the aerodynamic performance is lower, it is crucial to control of flow and to generate higher lift for this kind of vehicles, devices and/or creatures.

2. Transition

Transition is the phenomenon which occurs in trough different mechanisms in different applications (Langtry & Menter, 2006). The strongest factors affecting transition process are roughness of the wall or surface where the flow passes, adverse pressure gradient and freestream turbulence (Uranga, 2011). Transition is categorized as natural transition, bypass transition, separated flow transition, wake induced transition and reverse transition. There is a parameter to anticipate the type of transition. This parameter is called as acceleration parameter, which represents the effect of freestream acceleration on the boundary layer. The acceleration at the beginning of transition is defined as $K = (v/U^2)(dU/dx)$ (Mayle, 1991). Figure 2 (Mayle, 1991), from which one can decide the type of transition, is plotted as acceleration parameter versus momentum Reynolds number. Above the line marked "*Stability Criterion*" Tollmien-Schlichting type of instability is possible. The separation of a laminar boundary layer occurs above the line marked "*Separation Criterion*". The separation may lead to a separated flow transition. The shaded region on Figure 2 corresponds to the transition Reynolds numbers for turbulence levels between 5% and 10%.

Mayle (1991) presented a study of laminar to turbulent transition phenomena, types of transition and their effects on aerodynamics of gas turbine engines and he also reviewed both theoretical and experimental studies. Schubauer & Skramstad (1947) studied on a flat plate and showed the boundary layer is laminar at local Reynolds numbers (Re_x) lower than 2.8×10^6, whereas the boundary layer is turbulent when Re_x is higher than 2.8×10^6. The boundary layer at Re_x numbers between these two values is called as transitional boundary

layer. Formation and type of transition depend on airfoil shape, angle of attack, Re number, free stream turbulence intensity, suction or blowing, acoustic excitation, heating or cooling (White, 1991).

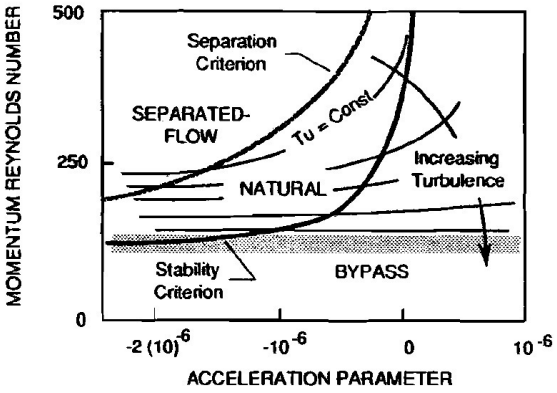

Fig. 2. Topology of the different types of transition in a Reynolds number-acceleration parameter plane (Mayle, 1991)

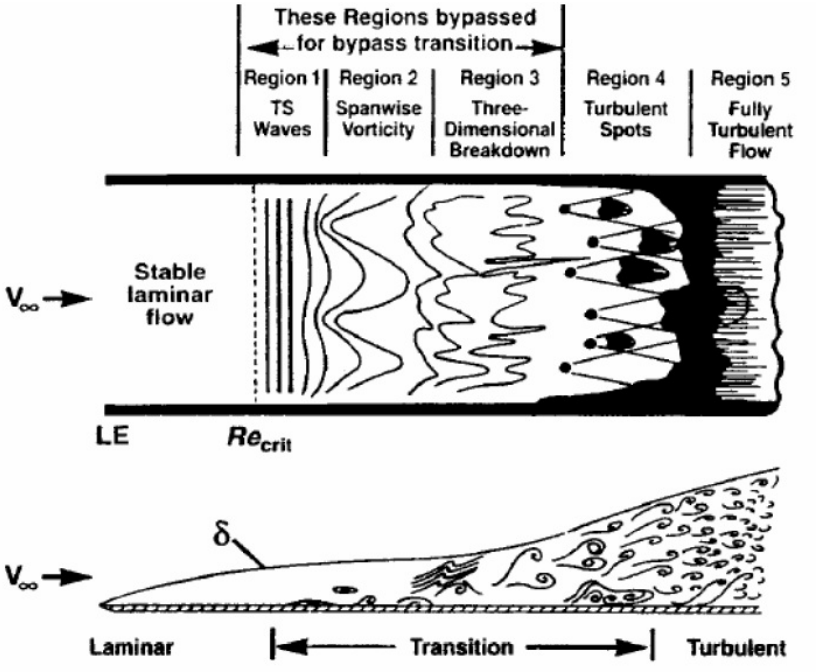

Fig. 3. The natural transition process (Schlichting, 1979)

2.1 Natural transition

This type of transition is seen at high Re numbers and low freestream turbulence levels. Natural transition begins with Tollmien-Schlichting (T/S) waves (Figure 3). T/S waves are the weak instabilities in the laminar boundary layer and this phenomenon was described first by Tollmien and Schlichting (Schlichting, 1979). In order to indicate the T/S waves, a quiet and a relatively less vibrant wind-tunnel and/or experimental apparatus must be employed, based on the fact that the T/S waves are weak instabilities and can be scattered at the higher freestream turbulence levels so freestream turbulence level must be low (<1% (Mayle, 1991)) to observe the T/S waves. Viscosity destabilizes the T/S waves and the waves start to grow very slowly (Langtry & Menter, 2006). The growth of the weak instabilities mentioned, results in nonlinear three-dimensional disturbances. After this certain point the three-dimensional disturbances transform into turbulent spots (Figure 4). The turbulent spots combine and so transition from laminar to turbulent is completed, from now on the flow is fully turbulent. Emmons (1951) and Emmons & Bryson (1951) stated that the turbulent spots within the boundary layer grew and propagated downstream until the flow was fully turbulent. They also presented a model of growth mechanism of turbulent spots, which indicated the time and location dependent random production of the spots.

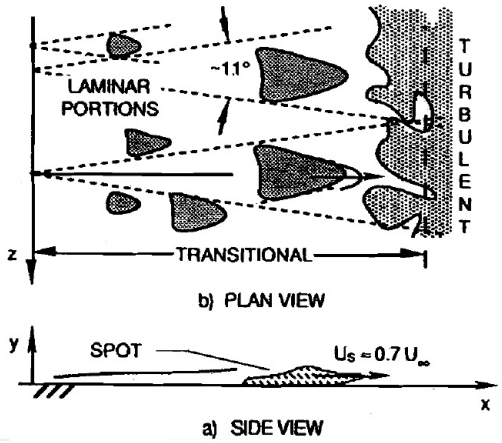

Fig. 4. Turbulent spot geometry and emergence of a turbulent boundary layer trough the growth and propagation of turbulent spots (Mayle, 1991)

2.2 By-pass transition

The other type of transition is bypass transition. As the name suggests, for this type of transition, first, second and third stages of the natural transition process are bypassed (Figure 3). Bypass transition occurs at flows having high freestream turbulence levels. The stages mentioned are bypassed and the turbulent spots are directly produced within the boundary layer by the influence of the freestream disturbances (Mayle, 1991). For bypass transition, linear stability theory is irrelevant and T/S waves have not been documented yet when the freestream turbulence is greater than 1% (Mayle, 1991). So the value 1% can be taken as the boundary between natural and bypass transitions. Lee & Kang (2000) investigated the transition characteristics in a boundary layer over a NACA0012 aerofoil by means of hot-wire

anemometry at a range of Reynolds number of $2x10^5$ and $6x10^5$. The aerofoil installed in the incoming wake generated by an aerofoil aligned in tandem with zero angle of attack. The gap between two aerofoils varied from 0.25 to 1.0 of the chord length. Consequently, they pointed that bypass transition occurred in flows around an aerofoil when incoming wave was turbulent and when the incoming wake was present, the transition onset shifted upstream and the transition length became smaller as Re number increased and as the aerofoil gap decreased.

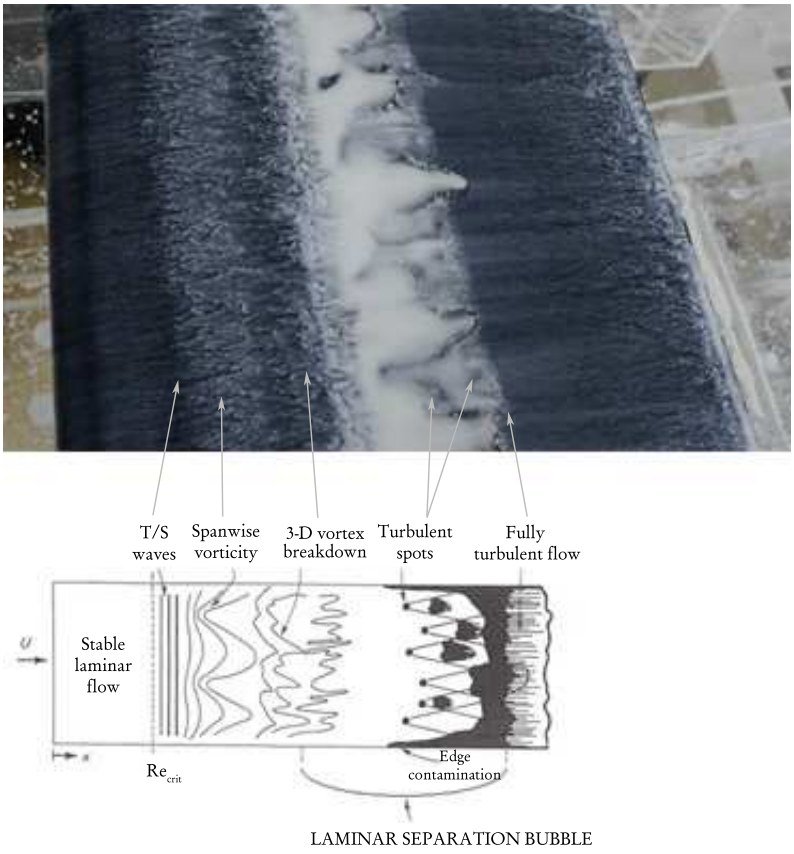

Fig. 5. Comparison of schematic of separation-induced transition process with the experimental photograph obtained oil-flow visualization over the NACA2415 aerofoil (Genç et al., 2012)

2.3 Separated flow transition

At high Re numbers, the laminar boundary layer on an object may transit to turbulent rapidly, and in most cases of high Re number aerodynamics applications, the boundary layer is able to overcome an adverse pressure gradient with minimum disturbance (Tan & Auld, 1992). For

low Re number aerodynamics, most of the experimental data indicates the occurrence of flow separation and reattachment in the transitional region (Burgmann et al., 2006; Gaster, 1967; Genç et al., 2008; Genç, 2009; Genç et al., 2011; 2012; Hain et al., 2009; Karasu, 2011; King, 2001; Lang et al., 2004; Mayle, 1991; Mohsen, 2011; Ol et al., 2005; Ricci et al., 2005; Swift, 2009; Tan & Auld, 1992; Tani, 1964; Yang et al., 2007; Yarusevych et al., 2007). The volume full of slowly recirculating air in between the points of separation and reattachment is called *Laminar Separation Bubble* or *Turbulent Reattachment Bubble* (Mayle, 1991).

When a laminar boundary layer cannot overcome the viscous effects and adverse pressure gradients, it separates and transition may occur in the free-shear-layer-like flow near the surface and may reattach to the surface forming a LSB (Mayle, 1991). Flow in the region under the LSB, slowly circulates and reverse flow occurs in this region. The LSB may involve all the stages mentioned for natural transition (Mayle, 1991), but with a LSB stage having the slowly circulating flow region as shown in Figure 5. Genç et al. (2012) carried out experimentally detailed investigation on the LSB over NACA2415 aerofoil by means of oil-flow visualization, pressure measurement and hot-wire anemometry. They compared the flow pattern with the schematic of natural transition introduced by White (White, 1991) and rearranged the figure to adapt the schematic to separated flow transition (Figure 5 and 6).

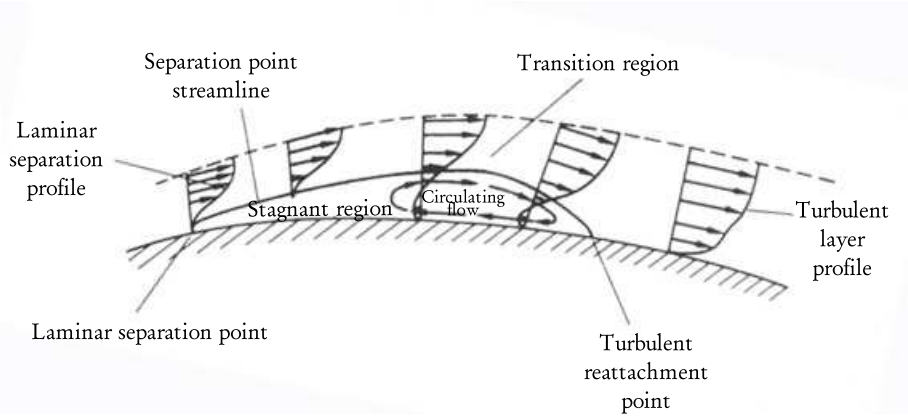

Fig. 6. Laminar separation bubble (Lock, 2007)

Laminar separation bubble may cause adverse effects, such as decreasing of lift force, increasing of drag force, reducing stability of the aircraft, vibration, and noise (Nakano et al., 2007; Ricci et al., 2005; 2007; Zhang et al., 2008). Characteristics of LSB must be understood well to design control system to eliminate to LSB or design new aerofoils which do not affect from adverse effects of LSBs. If Figure 7 (Katz & Plotkin, 1991) is examined carefully, a hump is seen on pressure distribution, this region illuminates the LSB, the region just after the maximum point of this hump indicates transition. If the flow is inviscid, LSB will not take place over the aerofoil.

In a favorable gradient (Figure 8a) the profile is very rounded and there is no point of inflection so separation cannot occur for this case and laminar profiles of this type are very resistant to a transition to turbulence. In a zero pressure gradient (Figure 8b), the point of inflection is at the wall itself. Separation cannot occur here either. The flow will undergo transition at local Reynolds numbers lower than $Re_x = 3x10^6$. In an adverse pressure gradient (Figure

8c to 8e), a point of inflection occurs in the boundary layer. The distance of the point of inflection from the wall increases with the strength of the adverse pressure gradient. For a weak pressure gradient (Figure 8c), flow does not actually separate, but it is vulnerable to transition to turbulence at low Re_x numbers as low as 10^5. For a moderate pressure gradient a critical condition is reached where the wall shear is exactly zero ($\partial u/\partial y$=0). This is defined as the separation point (τ_w=0), because any stronger gradient will actually cause reverse flow at the wall. In this case the boundary layer thickens greatly and the main flow breaks away, or separates from the wall (White, 2004).

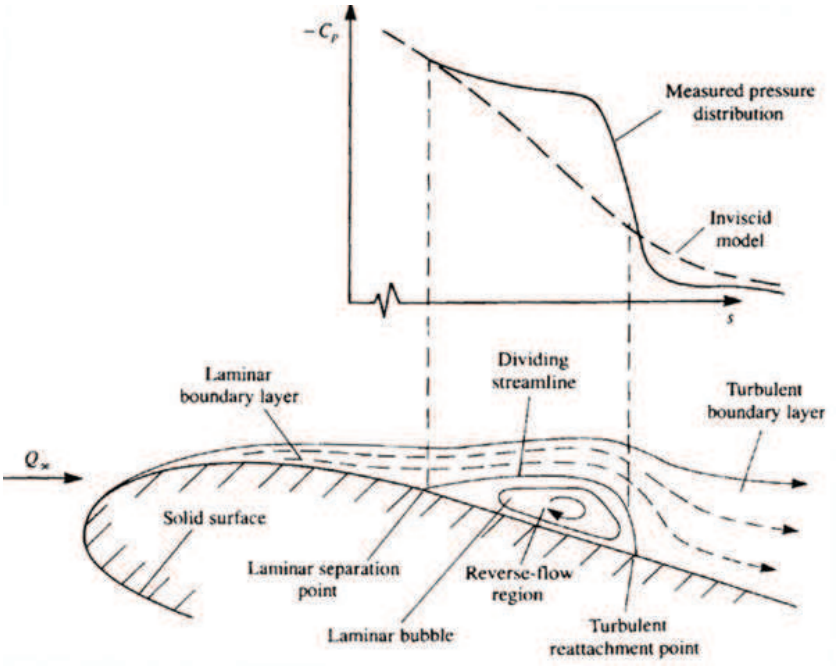

Fig. 7. The effects of laminar separation bubble on pressure distribution (Katz & Plotkin, 1991).

LSBs can be classified as short and long bubbles. The location and size of the bubble is a function of aerofoil shape, angle of attack, freestream disturbances and Re number (Swift, 2009; Tani, 1964). The LSB moves forward and contract in streamwise extent by the increase in angle of attack, which is classified as a short bubble (Tani, 1964). Within this kind of bubble, a small region of constant pressure can be seen, which causes a plateau in the curve of pressure distribution. In consequence of reattachment the curve of the pressure distribution recovers. As the angle of attack increases further, the separation point continues to move towards the leading edge and at a certain angle of attack the flow can no longer reattach to the aerofoil surface within a short distance. This phenomenon is called breakdown or burst of bubble. The occurrence of the breakdown phenomenon does not lead the flow to separate completely. The separated flow passes above the aerofoil and reattaches farther down-stream. The flow region under the separated flow slowly circulates and is called dead-air region or a long bubble. The presence of a short bubble does not significantly alter the peak suction. However, the presence of a long bubble results in a suction plateau of reduced levels in pressure distribution

(Figure 9) over the region occupied by the long bubble and does not result with a sharp suction peak (Tani, 1964). Tan & Auld (1992) experimentally investigated the flow over a Wortmann FX67-150K aerofoil at various Re numbers and various turbulence levels. They concluded that short separation bubbles formed at mild pressure gradient, and that as the pressure gradient increased the short separation bubble burst, forming a long separation bubble. In their experiments, they observed the reattachment of the flow shortly after the transition for the short separation bubble case. But for the long separation bubble case, the separated flow couldn't reattached to the aerofoil surface that quickly. They also stated that if the turbulence level of the freestream increased, length of the bubble decreased because of high energy of the flow, moreover for the short bubble case, the maximum turbulence intensity occurred in the region of reattachment where as the maximum value occurred much forward in the bubble.

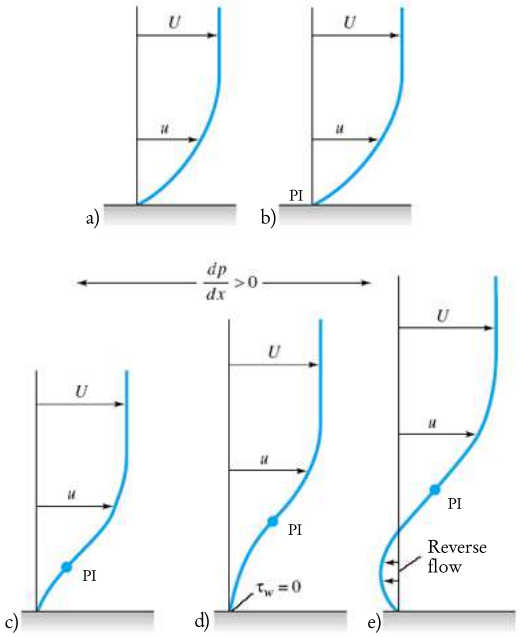

Fig. 8. The effects of various types of pressure gradients on boundary layer (White, 2004)

If the Re number is sufficiently low the separated flow may not reattach to the surface at all, so the laminar separation bubble will not be formed. Therefore the bubble formation is possible only for a certain range of Re numbers. The absence of a bubble at low Re numbers reduces the aerodynamic performance (Tani, 1964). There is a region above the upper surface of the detached flow and near the trailing edge, where the velocity is low and the flow reverses direction in places in a turbulent motion. As the angle of attack increases further, the beginning of the separation moves towards the leading edge of the aerofoil. At a certain angle of attack the lift rapidly falls off as the drag force rapidly increases. This phenomenon is called trailing edge stall. This type of stall is generally encountered on thick aerofoils and often refered as mild stall (McCullough & Gault, 1951). The other type of stall is leading edge stall, and leading edge stall is abrupt (Tani, 1964) laminar flow separation near the leading edge, generally without reattachment and can be encountered for aerofoils with moderate

thickness (McCullough & Gault, 1951). For the trailing edge stall the stalled state begins just after the highest lift force obtained. Thin-airfoil stall results from leading edge separation with progressive rearward movement of the point of reattachment. This type of stall occurs on all sharp edged aerofoils and on some thin rounded leading edged aerofoils (McCullough & Gault, 1951).

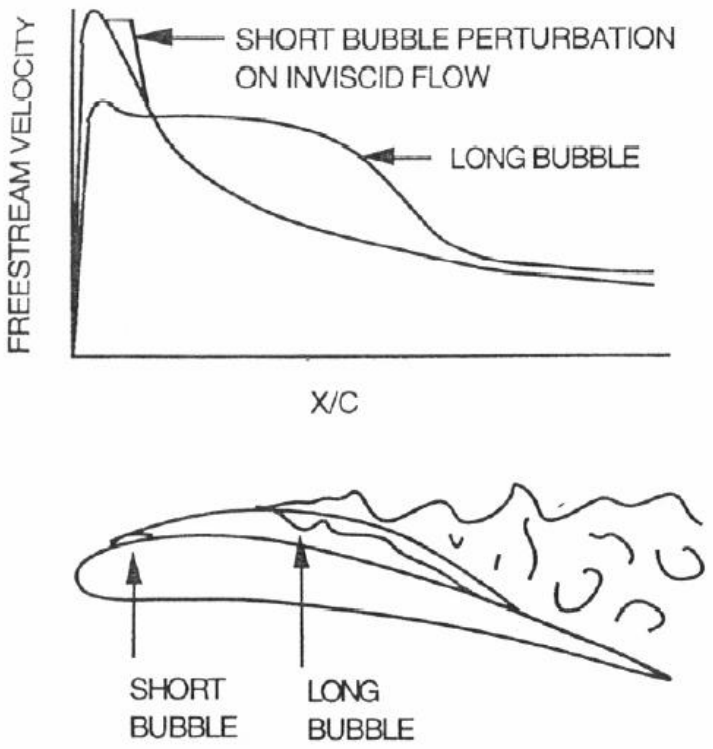

Fig. 9. Separation bubble effects on suction side velocity distribution (Langtry & Menter, 2006)

The effects of different types of stall on the lift coefficient can be seen on Figure 10 (Bak et al., 1998). The angle of attack, Re number, surface roughness and the aerofoil shape influence the stall phenomenon. Yarusecych et al. (2007) investigated NACA0025 aerofoil at a range of Re numbers of 0.55×10^5 to 2.1×10^5 and at three angles of attack (0°, 5° and 10°), by means of smoke-wire flow visualization and they observed two boundary layer flow regimes. At $\alpha = 5°$ and $Re=0.55 \times 10^5$ (Figure 11) the boundary layer on the suction surface of the aerofoil separated and the separated shear layer could not reattach. However, for angle of attack of 5° and $Re=1.5 \times 10^5$ the separated shear layer reattached and this formed a LSB.

(Gaster, 1967) performed an experimental study about LSB by means of constant temperature anemometry (CTA). This study was carried out over a wide range of Re numbers and in a variety of pressure distributions. The bursting circumstances of short bubbles were determined by a unique relationship between Re number and pressure rise. Consequently, LSB was classified as short and long bubble. In the study of Genç et al. (2012), additionally

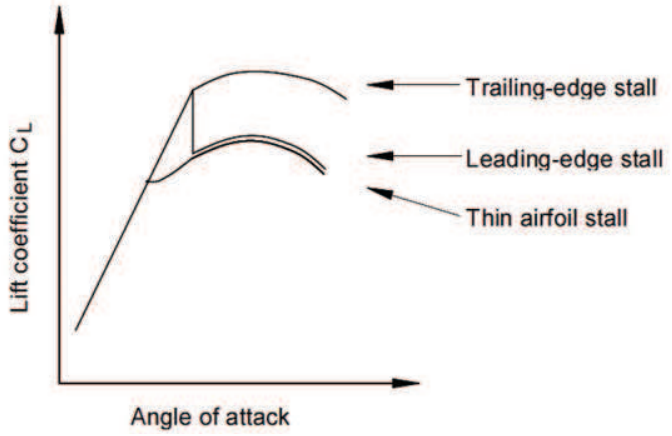

Fig. 10. Sketch of the three different stall types (Bak et al., 1998)

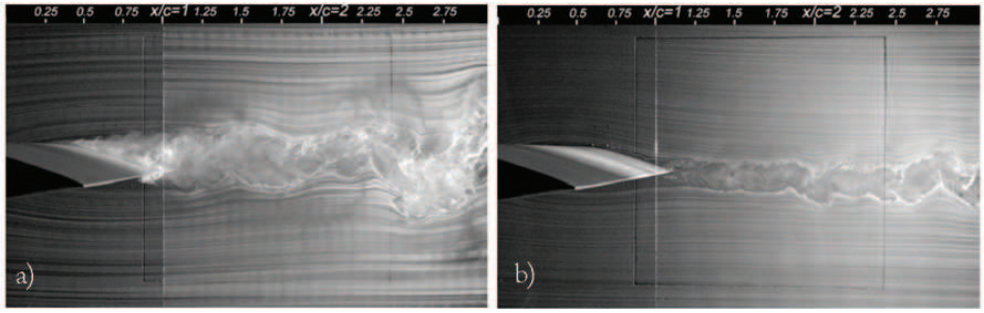

Fig. 11. Flow visualization results for NACA0025 aerofoil at a) Re=0.55x10^5 b) Re=2.1x10^5 (Yarusecych et al., 2007)

long bubble was seen at the angle of attack of 12° for Re=0.5x10^5 (Figure 12), this situation also indicates the bursting of the short bubble at $\alpha = 4°$ and $\alpha = 8°$ when the angle of attack reaches 12°, which leads to forming of a long bubble. The pressure distributions of the other angles of attack (4° and 8°), in which sharp suction peaks can be seen, indicate the presence of the short bubbles. In addition, Figure 12 points out that as the angle of attack increases the LSB moves towards the leading edge. Sharma & Poddar (2010) carried out an experimental study on NACA0015 aerofoil at low Reynolds numbers and at a range of angle of attack (-5° to 25°) and they used the oil flow technique to visualize the transition zone. They obtained the result that as the angle of attack increased the laminar separation bubble moved towards the leading edge and then the bubble burst at a certain angle of attack. The bursting of the bubble caused abrupt stall to occur. Long bubbles should be avoided since they produce large losses and large deviations at higher angles of attack. Short bubbles are effective way of forcing the flow to be turbulent and control the performance. However, one cannot easily predict whether the bubble will be long or short (Mayle, 1991).

Rinioie & Takemura (2004) conducted an experimental study on NACA0012 aerofoil at Re=1.35x10^5 and they concluded that, short bubbles are formed when the angle of attack was less than 11.5°, and long bubbles are formed when the angle of attack is higher than 11.5°.

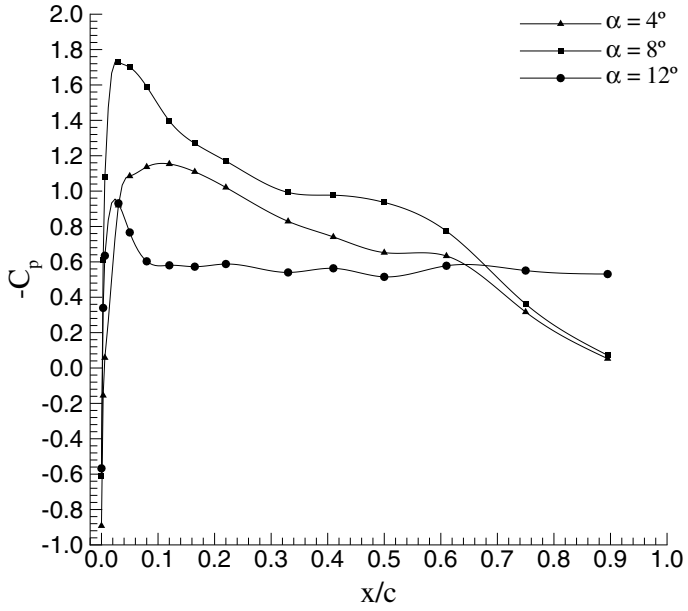

Fig. 12. C_p distributions over the NACA2415 aerofoil at different angles of attack for Re=0.5x10^5 (Genç et al., 2012)

Tan & Auld (1992) experimentally investigated Wortmann FX67-150X aerofoil at low Reynolds numbers and they obtained that as the Reynolds number and freestream turbulence intensity increased, transition occurred earlier and this caused the length of the laminar separation bubble to shorten. Yang et al. (2007) carried out an experimental investigation on GA(W)-1 aerofoil at varying low Re numbers. It was concluded that while the maximum length of the bubble was 20% of the chord length and the maximum height of the bubble was only 1% of the chord length. And also they pointed out that the unsteady vortexes induced by laminar separation bubble were caused by Kelvin-Helmholtz instabilities at angles of attack more than 7°. Diwan & Ramesh (2007) investigated experimentally the length and height of the LSB on a flat plate at different Re numbers. It was obtained that both length and height of the LSB decreased, and reducing ratio of the length is more than that of the height as Re number was risen. Hain et al. (2009) introduced the dynamics of the laminar separation bubbles on low-Reynolds-number aerofoils. It was obtained that Kelvin-Helmholtz instabilities had a weak effect in the spanwise direction and in the later stages of transition these vortices led to a three-dimensional breakdown to turbulence. Lang et al. (2004) also showed that transition in laminar separation bubble was driven by amplification of 2-D T/S waves and first stages of the 3-D disturbances played minor role in transition by studying both experimentally and numerically over an elliptical leading edged flat plate. Furthermore, the results showed that bidirectional vortexes lead to 3-D breakdown. Burgmann et al. (2006) conducted an experimental study on the flow over SD7003 aerofoil which used as wind turbine blades at low Re numbers by means of PIV. They stated that the shear roll-up in the outer region of the LSB causes the regions of concentrated vorticity to form. The vortex roll-up which was initialized by Kelvin-Helmholtz instabilities played effective role at transition process. The results showed that the quasi-periodic development of the large vortex-rolls had a convex or c-like

structure (Figure 13). They also mentioned that the c-like structures had no regular pattern in the spanwise direction and that these vortical structures interacted and disturbed each other and most of the vortices maintained their downstream speed, however some vortices decelerated which leaded to vortex-pairing. Their results also indicated that the vortices within the LSB formed as a consequence of the shear layer roll-up due to Kelvin-Helmholtz instabilities and these vortices peeled away from the main recirculation region. These vortices are tend to burst abruptly. The bursting of the vortices causes a strong vertical fluid motion from the wall into the freestream. They also stated that the vortex formed within the LSB increased in size and strength, and its downstream drift speed reduced this low speed state caused instability. The unstable low speed state leaded to a critical condition determined by the accumulation of the vortex strength assumed to be dominated by the momentum ratio and the vortex rotated as a whole structure around the reattachment point in the downstream direction. This leaded to strong ejection of low speed fluid into the freestream. This process acted as a local flow disturbance. The results also showed that the curvature of the aerofoil surface had a distinct effect on the development of the vortices.

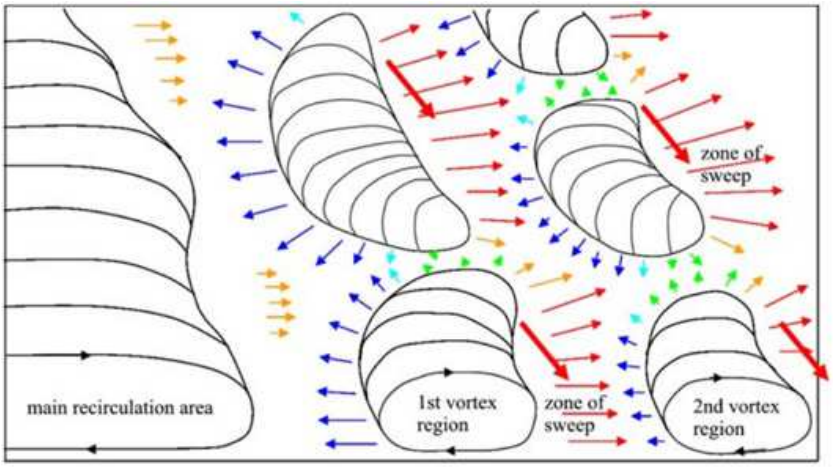

Fig. 13. Sketch of vortex footprint and convex vortex structures (Burgmann et al., 2006)

2.4 Reverse transition

This type of transition is the transition of turbulent to the laminar flow. This is called reverse transition or relaminarization. The relaminarization occurs because of the higher accelerations on the pressure side of most airfoils near the trailing edge, in the exit ducts of combustors and on the suction side of turbine airfoils near the leading edge (Mayle, 1991). Reverse transition is known to occur when the acceleration parameter (K) is greater than $3x10^{-6}$ (Mayle, 1991) and it is also possible for a relaminarized boundary layer to back to turbulent flow if the acceleration is small enough ($K<3x10^{-6}$).

2.5 Wake induced transition

Wake induced transition is an instance of the bypass transition which arises in turbomachinery flows where the blade rows subjected to periodically passing turbulent wakes (Langtry &

Menter, 2006). The experimental results showed that the wakes are so disruptive to the laminar boundary layer that turbulent spots often form in the region where the wake is first encountered the aerodynamic body (Langtry & Menter, 2006).

3. Transition modeling

The experimental systems, especially for flow control methods, are expensive and complex. Repeating experiments for a wide range of parameters will naturally cause very expensive solutions. Thus, numerical experimentations using range of CFD methods such as Reynolds Averaged Navier-Stokes (RANS) and/or Direct Numerical and/or Large Eddy Simulation (DNS/LES) methods arise as viable alternatives to experimentation. Furthermore, nowadays with advances in computing technology the CFD methods are used commonly. By using CFD, one can obtain the aerodynamic forces, pressure and velocity distributions over an aerodynamic body and can fix and/or improve the aerodynamic system before the final experimental test (Genç, 2009). Thus, the costs of experimental and design can be decreased.

In parallel with modern developments in experimental capturing, measuring, and identifying the LSBs that are typical for the low-speed flow regimes, improved prediction methods have been devised to account for transition mechanisms over wings of aeroplanes. Today, high performance computing capabilities make it possible to routinely use RANS based CFD methods for simulating low Re number flows. The RANS solvers frequently include practical one- or two-equation turbulence closure models (Wilcox, 1998) for turbulence calculations, although numerical transition modeling side still embed certain difficulties in capturing the complex transition process. Despite the difficulties, transition predictions have developed by means of the e^N method (Cebeci et al., 1972; Drela & Giles, 1987), two-equation low Re-number turbulence models (Cebeci et al., 1972), and some early (Drela & Giles, 1987) and modern (Abu-Ghannam & Shaw, 1994; Wilcox, 1994) methods based on experimental correlations. The e^N method has been quite successful in practice and more or less has become the industry standard (Cebeci et al., 1972). Standard two-equation low-Re models have shown certain successes although the wall damping terms' ability to capture important transition effects limits their use. The correlation-based models (Abu-Ghannam & Shaw, 1994; Suzen & Huang, 2000; 2003) have become helpful tools for industry owing to their use of integral (or global) boundary layer parameters. Recently, transport equation models (Fu & Wang, 2008; Langtry & Menter, 2005; Menter et al., 2004; Walters & Leylek, 2004; 2005) which rely on local information to circumvent some complex procedures in the early methods, have been introduced. These transport equation models solve several transport partial differential equations written for various transition quantities in addition to the baseline turbulence models. Some of these models have been made available in a number of commercial CFD codes such as FLUENT, ANSYS CFX (Langtry & Menter, 2005; Menter et al., 2004). Some of these models are the intermittency transport equation models of Suzen and Huang Suzen & Huang (2000; 2003) and the correlation-based k-ω Shear Stress Transport (SST) transition model of Menter et al. Menter et al. (2004). More recently truly single point RANS approaches such as the k-k_L-ω transition model of Walters and Leylek Walters & Leylek (2004; 2005) which essentially eliminates the need for the intermittency, and a variant of the SST model called as the k-ω-γ model of Fu and Wang Fu & Wang (2008) have been introduced. Such models are suitable for straightforward implementation within RANS methods as they solve additional transport equations for predicting transition phenomena that rely on local information only, in contrast with the global information, as used in the early methods. Assessment of these models has been recently made by different authors including trials of different user-dependent transition

correlations (Cutrone et al., 2008; Genç et al., 2008; 2009; Genç, 2009; 2010; Genç et al., 2011; Karasu, 2011; Kaynak & Gürdamar, 2008; Misaka & Obayashi, 2006; Suluksna & Juntasaro, 2008).

Lian & Shyy (2007) conducted a numerical study over a rigid and flexible SD7003 aerofoil and and compared the results with experimental measurements. They investigated the models by coupling a Navier-Stokes solver, the e^N transition model and a Reynolds-averaged two-equation closure to study the laminar separation bubble and transition. Also they proposed a new intermittency function suitable for low Re number transitional flows incurred by laminar separation. They concluded that the LSB became shorter and thinner with the increase of angle of attack. Also higher freestream turbulence levels caused a shorter and thinner separation bubble. And they achieved a good agreement with the model they employed, which is based on linear stability analysis and is designed for steady-state flows with the assumptions that the initial disturbance is small and the boundary layer is thin. Windte et al. (2006) conducted on an experimental and numerical study to investigate LSB over SD 7003 aerofoil at Re=6x10^4. RANS model was used to validation of results of the experiments. They concluded that however both Menter's BSL-2L and Wallin model gave good result, Menter's BSL-2L model gave the best results at both laminar separation and C_L.

The k-ω SST transition model is based on two additional transport equations beyond k and ω: the first is an intermittency equation (γ- equation) that is used to trigger the transition process; and the second is the transition onset momentum thickness Reynolds number ($Re_{\theta t}$-equation) which is forced to follow experimentally-determined correlations with some lag. In this model, SST feature is linked to the transition model by coupling it with the k-ω SST turbulence model (Menter, 1994). Transition correlations are user dependent data retrieved from benchmark experiments obtained at different laboratories. A number of investigators have tried to develop their own correlations of the model parameters against different experimental cases (Cutrone et al., 2008; Fu & Wang, 2008) as the original parameter set remains proprietary (Menter et al., 2004). The k-k_L-ω model is considered as a three-equation eddy-viscosity type, which includes transport equations for turbulent kinetic energy (k), laminar kinetic energy (k_L), and specific dissipation rate (ω). This model, which is essentially a single-point technique, combines the advantages of the prior correlation methods and eliminates the need for intermittency. In this model, the turbulent energy is assumed in the near-wall region to be split into small scale turbulent energy, which contributes directly to turbulence production, and large scale turbulent energy, which contributes to production of laminar kinetic energy through the splat mechanism (Walters & Leylek, 2004; 2005). Walters and Leylek Walters & Leylek (2004; 2005) assumed that transition initiates when the laminar streamwise fluctuations are transported a certain distance from the wall, where that distance is determined by the energy content of the free stream, and the kinematic viscosity. As for the the wall boundary conditions, the k-k_L-ω transition model uses a Neumann type boundary condition which specifies the normal derivative of the function on a surface, whereas the k-ω SST transition model uses Dirichlet type wall boundary conditions which gives the value of the function on a surface (Genç et al., 2011). Recently, Cutrone et al. (2008) proposed to use a combination of the two conditions for ω in the case of separated flows. Catalano & Tognaccini (2010) conducted on a numerical study over SD 7003 aerofoil has Re=6x10^4. In this study, RANS and DNS approach were used. Menter's standart k-ω SST and k-ω SST-LR (Low Reynolds) model were used for RANS approach. Stall and LSB characteristics were predicted same so they concluded k-ω SST-LR could be used for LSB. Sanders et al. (2011) carried out numerical investigation over GH1R low pressure turbine aerofoil using three RANS model

and compared with experimental results had been performed before and they concluded that the newer transition model k-k_L-ω model gave better results thank-ω SST and Realizable k-ϵ models according to the experimental values.

4. Experimental techniques at low Reynolds numbers

The wind tunnel tests are crucial for investigations at low Reynolds numbers. In order to understand and improve the performance of low Reynolds number aerofoils, accurate wind tunnel tests must be performed. Since the low Reynolds number aerofoil performance is highly dependent of the laminar boundary layer (Mayle, 1991), low turbulence levels in the wind tunnel's test section are necessary (Selig et al., 2011). If the laminar boundary layer transitions to turbulent prematurely because of freestream disturbances, the phenomenon like laminar separation bubble may not be investigated and/or documented properly. In order to ensure low levels of freestream turbulence and good flow quality in test section of wind tunnel, turbulence screens and honeycombs may be employed. In order to determine aerodynamic characteristics of an aerofoil, wind tunnel test methods such as force and pressure measurements, velocity measurement by using a manometer and pitot static-tube system, hot-wire system and laser doppler anemometry (LDA), laser doppler velocimetry (LDV), and PIV, flow visualizations with oil, smoke wire may be done.

Pressure measurements: Pressure measurement is made by a device at rest relative to the flow. Pressure is usually measured both at walls and in the freestream using the types of measurement device such as pitot static-tube connected to a transducer or manometer. At walls, pressure tappings can be used and can be connected to pressure measurement device via tubes. In order to measure the pressure, one or more transducers can be employed. When a transducer is employed, calibration system requires and calibration can be carried out using by a manometer and pitot-static tube.

Force measurements: During the early years of wind tunnel testing, forces and moments were measured through pan-type *balances*. Although technology has gradually developed, the term *balance* is still used to the devices used for force and moment measurements, today. Balances can be divided into two main groups as internal and external. These names are derived from their location relative to the test model and wind tunnel test section. Internal balances which are almost universally used for measurements in supersonic and transonic tunnels locate inside a model, while external balances which are used in subsonic wind tunnels locate outside the test section of wind tunnel. External balances are with either three or six components. Three-component balances measure lift, drag and pitching moment while six-component balances also measure side force, rolling moment and yawing moment. In external balances, load cell systems are employed. Load cells which simply measures the deformation can be placed on a rod weakened in different axis for different forces and moment. When the wind tunnel is on the weakened part of the rod for the each force will undergo deformation and with the load cells placed on each part one can obtain the data for forces and moment. A balance system software, which is calibrated for forces and moment, gives digital output of forces and moments in desired units. The calibration is performed by loading the load cell with known weights and is repeated before each set of experiments to ensure consistency (Genç et al., 2012).

Velocity measurements: Velocities and turbulence intensities for different points and fields around an object can be measured by using a manometer and pitot-tube system, hot-wire system, and LDV, LDA and PIV. Measurement by using a manometer and pitot-tube system is

pressure-based velocity measurement and this method is related to measurement of dynamic pressure. Then, the velocity is calculated with dynamic pressure measured by using Bernoulli equation. This method is simple and inexpensive. The hot-wire system is the most used system, for their very small probes, low response time and high precision for measuring velocity components and turbulence characteristics. This system is capable of detecting turbulent fluctuations with a large dynamic response because of the very small hot-wire thermal inertia and its correction in the anemometer. The hot-wire system can be operated in three methods: constant current (CCA), constant temperature (CTA) and constant voltage (CVA). This systems require also calibration techniques and electronic circuit consisting of a Wheatstone bridge. The probe of a hot-wire system consists of an electrically heated a wire or a thin film. Usually the wire of the probe is made of tungsten or platinum, 0.5-2 mm long and has a diameter of 0.5-5 μm. The films are about 0.1 μm thick and deposited on fine cylinders of quartz, about 25-50 μm in diameter.

Genç et al. (2012) investigated the characteristics of NACA2515 aerofoil at Re numbers of $5x10^4$, $1x10^5$, $2x10^5$ and $3x10^5$ and varying the angle of attack from -12° to 20°. The separation, transition, the formation and progress of the laminar separation bubble and reattached flow were observed obviously by means of force measurements, constant temperature anemometry and pressure measurements. They pointed out that, the near highest point of the peak in the pressure coefficient of suction surface indicated the transition from laminar to turbulent flow and the fluctuations in the graphs of force and moment denoted the separation a post-stall. The C_L-α curves showed that the stall angle and the stall abruptness increased as the Reynolds number raised. Selig et al. (2011) presented a study of a flapped AG455ct aerofoil and a flat-plate with leading edge serration geometries (protuberances like those found on fins/flippers of some aquatic animals) to explore the effects on stall characteristics at low Re numbers and varied angles of attack by means of force measurements. The results for the flapped AG455ct aerofoil showed a dramatic increase with higher flap deflections and the flap efficiency reduces with large deflections up to 40°. And the tests on the flat-plate aerofoil with leading edge serration geometries showed that the serrations on the leading edge lead to higher lift and softer stall and lower drag in the stall and post-stall.

Optical Measurement Techniques: LDV, LDA and PIV techniques are particle-based and optical measurement techniques. These techniques rely on the presence of tracer or seed particles in the flow which not only follow all flow velocity fluctuations but are also sufficient in number to provide the desired spatial or temporal resolution of the measured flow velocity. In these sytems, laser is used to illuminate the desired plane. The laser sheet is placed based on the plane in which velocity will be measured. A combination of cylindrical and spherical lenses is used to adjust both the thickness and the width of the laser sheet. Images are captured using a camera, and a cross-correlation algorithm is used to analyze the images and to calculate the velocities. Ol et al. (2005) compared three different facilities for investigating the LSB on SD7003 aerofoil at low Re number by means of PIV. They conducted experiments in a tow tank, a low-noise wind tunnel and a free-surface water tunnel at Re number of $6x10^4$ and angles of attack of 4°, 8°, 11°. The results showed a qualitative similarity in the bubble shape and velocity fields, as well as the Re stress distributions but the measured location and flow structure of the bubble was still contradictory.

Flow Visualization: Flow visualization is the way to visualize and understand the characterization of the flow. However, air and water which are both used in experiments are transparent, and the observer cannot see the flow and the streamlines around an object with naked eye. So, to make the flow visible, there are two different principles. One is to add

different substances into the flow. These substances must be small enough to be able to follow the flow and large enough to be seen. The other principle is to alter the optical properties of the flow. The ratio of refraction of the light passes through the fluid media is a function of the density of the fluid. So within compressible flow, the flow field can be made visible by changing the refractive ratio of light passes through the fluid media (Genç, 2009).

There are different techniques of flow visualization, both optical and by adding different substances. These are smoke visualization, surface flow visualization and optical methods. The smoke visualization method is made by using a smoke-wire or a fog generator. A fog generator usually, generates a single strip of smoke. This may be a disadvantage because, one cannot easily visualize the flow within a large area with just one strip of smoke. The advantage of this method is that the fog generators usually use odorless, non-toxic oil to generate fog. A smoke wire is a high resistant wire or a coil of wires which is stretched between the walls of a wind tunnel and coated with oil. When voltage applied to the smoke wire the wire, gets hot and the oil starts to evaporate to create short bursts of smoke filaments, marking streak lines (Yarusevych et al., 2008a). These filaments introduced to the flow can easily mark the separation and the bubble. To document streak lines, separation and bubble a high-speed camera can be employed for digital imaging (Yarusevych et al., 2008a). As the Reynolds number increases, it gets harder to get a proper image owing to the decrease of smoke filaments' duration. Smoke wire diameter, voltage and the coating liquid employed may be changed as the Reynolds number increases or decreases (Dol et al., 2006). The number of smoke droplets per unit length of the wire depend on the wire diameter and the surface tension of the coating liquid. And also the smoke duration depends on voltage and droplet size (Torii, 1977). This method may not be adequate for higher Reynolds numbers because of being constrained by the smoke duration (Dol et al., 2006; Mueller, 1983; Yarusevych et al., 2008a). (Dol et al., 2006) studied experimentally to determine the optimum smoke-wire material and diameter, wire design (single or coiled), and coating liquid for varying freestream velocities. They concluded that Safex is the most effective liquid and two-coiled Nichrome wire is the optimum wire design to use at freestream velocity of 2 m/s. Yarusevych et al. (2008a) studied experimentally on a NACA0025 aerofoil at low Reynolds numbers by means of smoke-wire visualization and obtained images with a high speed camera. They employed a wire of 0.076 mm diameter and applied 100 volts of voltage to electrically heat and evaporate the coating oil. And they concluded that at $Re_c = 5.5 \times 10^4$ the vortices appeared to form a pattern in the wake region of the aerofoil (approximately, x/c=1 and x/c=2) were similar to a Karman vortex street. Yarusevych et al. (2008b) investigated also the vortex shedding characteristics on a NACA0025 aerofoil at low Reynolds numbers and three different angles of attack by means of constant temperature anemometry and smoke-wire flow visualization method. And they concluded that the shedding frequency of the shear layer roll-up vortices was found to exhibit a power law dependency on the Reynolds number; whereas, the wake vortex shedding frequency varied almost linearly with the Reynolds number. However, the results demonstrated that these correlations depend significantly on the shear layer behavior. Moreover, in contrast to flows over circular cylinders, the ratio of the two frequencies did not exhibit a power law dependency on the Reynolds number.

Yarn tufts (Figure 14) are applied to the surface of the aerofoil and they are used for indicating the flow pattern on the surface of the aerofoil when the wind tunnel is on. They are easily applied to any surface and can be used at any model position. But they do not provide a detailed flow pattern due to moving constantly with the airflow (UWAL, 2012).

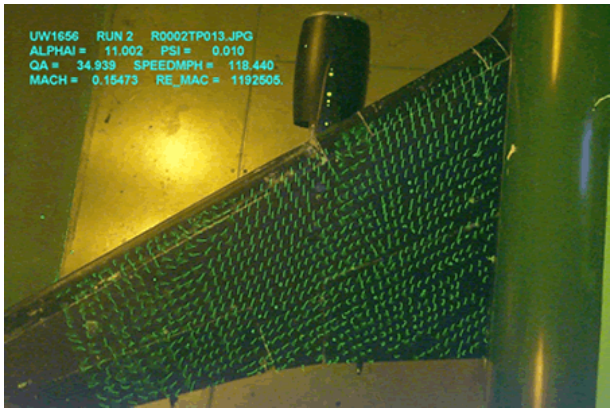

Fig. 14. Fluorescent mini-tufts on an aircraft wing (UWAL, 2012)

Oil-flow surface visualization method is a simple and effective way of documenting the surface flow events by means of photography. In order to photograph the surface flow events using this method, the pigmented oil is applied into a mat black aerofoil and the wind tunnel is on (Genç et al., 2012). Once the oil on the aerofoil's surface is dried, the flow events on the aerofoil surface can be observed and photographed. But it is important to have the proper type of oil mixture for certain wind tunnel speed. The mix should have the right consistency to effectively indicate the development of the boundary layer (Genç et al., 2012). The inertia forces of the moving oil should be lower than the viscous and surface tension forces (Merzkirch, 1974) in order to not affect the flow events on the surface. Some common oils are light diesel oil, light transformer oil and kerosene and some common pigments are titanium dioxide and china clay. Furthermore to see the pigment residue more clearly oleic acid can be added to the mixture (Genç et al., 2012). Genç et al. (2012) investigated experimentally the flow over NACA2415 aerofoil at low Reynolds numbers also by means of oil-flow surface visualization. They applied a mixture using titanium dioxide as pigment, kerosene as oil and oleic acid to see the flow pattern more clearly. They photographed and documented the laminar separation bubble at Reynolds numbers of $1x10^5$, $2x10^5$ and $3x10^5$ and at angles of attack of 4°, 8°, 12° and 15°, and compared the results with constant temperature anemometry and pressure measurements experiments. Consequently, they observed the formation and progress of the separation bubble and reattached flow clearly. Selig et al. (2011) studied on E387 aerofoil at low Re numbers by means of oil-flow surface visualization and sketched a graphic of relation between oil-flow visualization photograph and skin friction coefficient (Figure 15). They also mentioned that the texture that existed before running the tunnel still existed in the leading-edge region of the LSB due to the stagnant flow, and that the magnitude of the C_f in this region is quite small because of the low flow speed, and negative in sign because of the reverse flow.

5. Flow control at Low Reynolds numbers

The concept of boundary layer control was introduced first by Prandtl (1904). Flow control methods can be categorized as active and passive flow control methods (Mohsen, 2011; Ricci et al., 2007). Active flow control can be made by adding energy to the free stream or to the boundary layer directly. Passive flow control can be carried out by adding geometrical

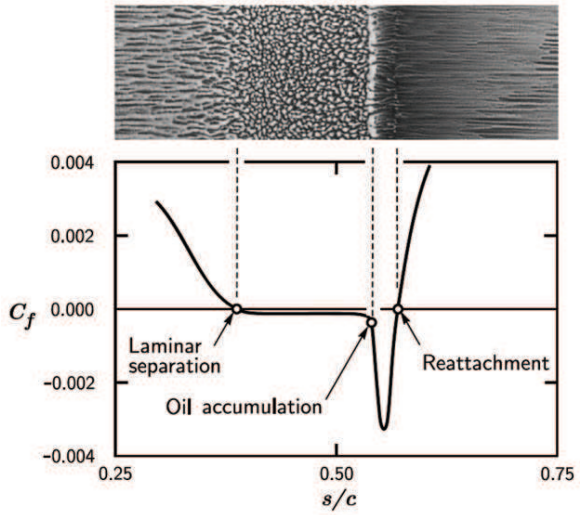

Fig. 15. Conceptual illustration of the relationship between the surface oil flow features and skin friction distribution in the region of a LSB (Selig et al., 2011)

discontinuities or increasing the roughness of the surface. Passive flow control may be simple and cheap but it has its own disadvantages. This kind of geometrical discontinuities increase the drag force and since they are fixed, they cannot adjust with the changing location of the LSB and off-design conditions (Mohsen, 2011; Ricci et al., 2007). Shan et al. (2008) carried out a numerical study on a NACA0012 aerofoil in three different cases. These are uncontrolled flow separation, flow separation control with passive vortex generators and flow separation with control with active vortex generators. And the results showed that in the case of flow separation control with passive vortex generator, the time and spanwise averaged results have shown that the separated flow in the immediate downstream region over an extent of 0.1C. However, the reattached flow separated again and in the conclusion of the transition and reattachment of the separated layer formed the second laminar separation bubble. Thus, the passive vortex generators reduced the size of the separation zone by approximately 80%. The results of the numerical investigation of the active vortex generators case there were no sign of separation so that the flow control with the active vortex generators is more effective than the passive ones. Lengani et al. (2011) investigated the effects of low profile vortex generators on a large-scale flat plate with a prescribed adverse pressure gradient. They placed the vortex generators in the meridional and cross-stream panels and surveyed the velocity fields by means of Laser Doppler Velocimetry (LDV) and measured the total pressure by means of a Kiel total pressure probe. They showed that the presence of vortex generators induced the cross-stream vortices to suppress the separation with large flow oscillations. Santhanakrishnan & Jakob (2005) presented a numerical investigation on a standard Eppler 398 aerofoil with regular perturbations at a range of Re numbers, 2.5×10^4 to 5×10^5. They used smoke-wire flow visualization for qualitative observation of both perturbed and unmodified aerofoils to determine the region of separation. They also employed 2-D PIV measurements to understand the near-wall flow-field behavior. Consequently, at $Re=2.5 \times 10^4$ and $\alpha=4^\circ$, separation started very close to the leading edge of the unmodified aerofoil and there was no reattachment. But for the perturbed aerofoil, the flow was attached and the point of

the separation was moved further downstream due to the addition of the perturbations. Dassler et al. (2010) developed a new approach for modeling the roughness induced transition, which based on local variables and a transport equation. Two functions determining the value of the transported variable named roughness amplification (Ar), are employed in this model. They implemented the model in the DLR flow solver TRACE and they validated the model by two test cases, a flat plate with roughness and different linear pressure gradients and a flat plate with a two-scale roughness. They indicated the shifting of the transition onset position when different surface roughness values and step change of roughness were prescribed and this result showed that the approach was feasible and was in agreement with the measurements. Roberts & Yaras (1947) conducted an experimental study on a flat surface with five variations. These are three different freestream turbulence intensities (0.5%, 2.5% and 4.5%) and two different Re numbers ($3.5x10^5$ and $4.7x10^5$). They observed both attached flow and separation flow transition with laminar separation bubble. They also mentioned that T/S instability mechanism was responsible for transition in each of the test cases. Consequently, for most of the range of surface roughness heights, the roughness elements remained below the transitioning shear layer of the bubble. This showed that, the roughness elements had no effect on the rate of transition. Ergin & White (2006) carried out an experimental study in a flat plate boundary layer downstream of a spanwise array of cylindrical roughness elements at both subcritical and supercritical values of Re_k. They observed rapid transition only for Re_k=334 because of the sufficiently large fluctuation growth, and they stated that the growth of unsteady disturbance increased with the increasing Re_k. However, for subcritical configurations these disturbances stabilized before the transition could occur. Rizetta & Visbal (2007) used DNS to investigate the effects of roughness elements on a flat plate, for roughness based Re numbers of 202 and 334, and they compared the numerical results with experimental results. The numerical method they employed used a sixth-order-accurate numerical scheme and an overset grid methodology for describing the computational flow-field and a high-order interpolation procedure was employed to maintain accuracy at overlapping boundaries of distinct mesh systems which used for defining the roughness element. For Re_k=202, growth of the integrated turbulent energy was displayed by the simulation in the streamwise extent of computational domain. They also stated that this behavior did not observed experimentally. For Re_k=334, explosive bypass transition displayed by the simulation. Cossu & Brandt (2002; 2004) studied the effect of three-dimensional roughness element in laminar boundary layer. The optimal disturbances in fixed finite magnitude is captured the boundary layer T/S disturbance. They investigated the effects of spanwise invariant disturbances in the T/S unstable frequency band on boundary layer. They found that the stationary finite-amplitude optimal disturbances could suppress the growth of the T/S-like disturbances in a boundary layer.

On the other hand active flow control methods, such as suction/blowing systems, may be expensive and complex but they can adjust with the changing location of the laminar separation bubble by changing the control parameters and/or off-design condition by completely switching of the whole control system. But for active blowing systems some additional disturbances may be generated by the secondary flow through the holes may still be present (Mohsen, 2011). Genç (2009) and Genç et al. (2008; 2009; 2011) studied the prediction of the LSB over the aerofoils at low Re numbers, and the controlling this LSB by using high lift (Genç et al., 2008; 2009; Genç, 2009), blowing and suction systems (Genç, 2009; Genç et al., 2011). The numerical results of the control cases, it was predicted that the separation bubble was eliminated by using the slat, blowing and suction resulting in some marginal increase in the lift and decrease in drag.

Acoustic excitation is an active flow control method, in which typically a signal generator, amplifier and a sound source were used (Ricci et al., 2007). The frequency of the sound wave introduced to the flow can be adjusted with the changing behavior of the aerodynamic body. Theoretically the acoustic excitation induces T/S waves forcing the transition to begin (Ricci et al., 2007). Ricci et al. (2005; 2007) conducted studies on the effects of acoustic disturbances on laminar separation bubbles by means of IR thermography at Reynolds number of $6x10^4$. They inspected a RR3823HL aerofoil at varied angles of attack between 2° and 8°. They introduced a sinusoidal sound wave frequency range was between 200 and 800 Hz with a step of 100 Hz. They concluded that the sinusoidal sound wave having certain frequency reduces the laminar separation bubble's length by retarding the separation. Yarusevych et al. (2007) studied the effect of acoustic excitation amplitude on boundary layer and wake development at low Reynolds numbers by means of hot-wire anemometry, pressure measurements and flow visualization. The results showed that an increase of the excitation amplitude advances the location of reattachment and delays boundary layer separation, reducing the extent of the separation region. Also they indicated that when boundary layer separation occurs without reattachment, the increase of the excitation amplitude above the minimum threshold leads a separation bubble formation with delayed boundary layer separation. Zaman & McKinzie (1991) investigated the effects of acoustic excitation in reducing the adverse influences of the LSB over two dimensional aerofoils at low angles of attack by using smoke wire visualization and hot wire anemometry. They studied in the chord based Re number range of $2.5x10^4 < Re_c < 1x10^5$. However the amplitude of the excitation-induced velocity fluctuation kept constant at a reference point within the flow field, it was founded that the most effective frequency scale was as ${U_\infty}^{3/2}$. The parameter $St/({Re_c}^{1/2}$ corresponding the most effective frequency for all of the cases studied falls in the range of 0.02 to 0.03, with Strouhal number based on the chord. Experimental results showed that lift coefficient had a significant improvement. Zaman (1992) also investigated the effects of acoustic excitation on post-stalled flows over an aerofoil. They used a two dimensional aerofoil LRN (1)-1007 with a chord length of 12.7 cm and employed a crossed hot-film probe for the experiments. The acoustic excitation resulted in a tendency to force the flow to reattach, which was accompanied by an increased lift coefficient and reduced drag coefficient. It was shown that as the amplitude of excitation was increased, a large enhance in the lift was achieved. Ishii (2003) presented the effect of weak acoustic excitation on a separated flow over an aerofoil. Two-dimensional numerical simulations are performed for an NACA0012 aerofoil at angle of attack of 12° and Reynolds numbers, $5x10^4$ and $1x10^5$. The amplitude of external sound pressure was set at %0.05 of the static pressure. Numerical results pointed that the acoustic waves with effective frequencies increased the time-averaged lift coefficients. Chang et al. (1992) studied on internal acoustic excitation on the improvement of $NACA63_3 - 068$ aerofoil performance at low Re numbers by means of hot wire and pressure measurements. The acoustic excitation by a loudspeaker was funneled into the interior of the model and then ejected into the flow field from a narrow slot of 0.6 mm in width at %1.25 chord from the leading edge. Experimental results indicated that the flow separation was delayed at the post-stall angle with a low level excitation.

6. Conclusion

In this study, a review of low Reynolds number flows was presented. Firstly, transition and transition types were explained. These transitions types are natural transition, by-pass transition, separated flow transition, reverse transition and wake induced transition. Natural transition is seen at high Reynolds number and low free stream turbulence level. Bypass transition is occurred at high freestream turbulence level and some phases of the natural

transition are bypassed. Wake induced transition is an instance of the bypass transition which arises in turbo-machinery flows where the blade rows subjected to periodically passing turbulent wakes. Reverse transition is transition from turbulent flow to laminar. The most important transition for low Reynolds number flows is separated flow transition, in which the flow separates from surface because of viscous effects and adverse pressure gradient, and transition process is completed in the separated region then the fully turbulent flow reattaches to surface. The region between the separation point and the reattachment point is called LSB, which causes negative effects such as decreasing performance, decreasing stability and early stall in aircrafts. LSBs are classified as long bubbles and short bubbles. If short bubble bursts or the separated flow can not reattach to surface and stall will occur and this is a serious problem for aerofoils. Thus, LSB occurring at low Re number flows must be controlled or delayed. Experimental techniques such as pressure measurement, velocity measurement, PIV, smoke and oil flow visualization can be applied for low Reynolds number flows, for instance if pressure distribution is obtained over an aerofoil, a hump is seen at region where laminar separation bubble takes place or another simple method to see LSB region is oil flow visualization method, since there is no movement inside the dead region of LSB, the oil applied before to surface does not move so separation and reattachment point can be seen clearly. Furthermore, transition modeling is one of the most popular research areas nowadays although it has not completely accomplished to model the low Re number flows yet.

7. References

Abu-Ghannam, B.J. & Shaw, R. (1980). Natural Transition of Boundary Layers-The Effect of Turbulence, Pressure Gradient and Flow History. *Journal of Mechanical Engineering Science*, Vol. 22, pp. 213-228.

Bak C., Madsen H.A., Fuglsang P., Rasmussen F. (1998). Double Stall, Risø National Laboratory Technical Report Risø-R-1043(EN), Risø National Laboratory, Roskilde, Denmark.

Burgmann, S., Briicker, C., Shroder, W. (2006). Scanning PIV Measurements of a Laminer Separation Bubble. *Experiments in Fluids*, Vol. 41, pp. 319-326.

Catalano, P. & Tognaccini, R., (2010). Turbulence Modeling for Low-Reynolds-Number Flows. *AIAA Journal*, Vol. 48, pp. 1673-1685.

Cebeci, T., Mosinskis, G.J. and Smith A.M.O. (1972). Calculation of Separation Points in Incompressible Turbulent Flows. *Journal of Aircraft*, Vol. 9, pp. 618-624.

Chang, R.C., Hsiaot, F.B., Shyu, R.N. (1992). Forcing Level Effects of Internal Acoustic Excitation on the Improvement of Airfoil Performance *Journal of Aircraft*, Vol. 29, No. 5, pp. 823-829.

Chklovski, T. (2012) Pointed-tip wings at low Reynolds numbers, University of Southern California, USA, $www - scf.usc.edu/ \sim tchklovs$, Access January 2012.

Cossu, C., Brandt, L.. (2002). Stabilization Tollmien-Schlichting waves by finite amplitude optimal streaks in the Blasius bounday layer. *Physics of Fluids*, Vol. 14, No. 8, pp. L57-L60.

Cossu, C., Brandt, L.. (2004). On of Tollmien-Schlichting waves in streaky boundary layers. *European Journal of Mechanics B/Fluids*, Vol. 23, No. 6, pp. 815-833.

Cutrone, L., De Palma, P., Pascazio, G., Napolitano, M. (2008). Predicting Transition in Two- and Three-dimensional Separated Flows. *International Journal of Heat and Fluid Flow*, Vol. 29, pp. 504-526.

Dassler, P., Kožulovic, D., Fiala, A. (2010). Modelling of Roughness-Induced Transition Using Local Variables. *V European Conference on Computational Fluid Dynamics*, 14-17 June 2010, Lisbon, Portugal.

Diwan, S.S. & Ramesh, O.N. (2007). Laminar separation bubbles: Dynamics and control. *SADHANA-Academy Proceedings In Engineering Science*, Vol. 32, pp. 103-109.

Dol, S.S., Nor, M.A.M., Kamaruzaman, M.K. (2006). An Improved Smoke-Wire Flow Visualization Technique. *Proceedings of the 4th WSEAS International Conference on Fluid Mechanics and Aerodynamics*, Elounda, Greece, August 21-23, pp. 231-236.

Drela, M. & Giles, M.B. (1987). Viscous-inviscid Analysis of Transonic and Low Reynolds Number Aerofoils. *AIAA Journal*, Vol. 25, pp. 1347-1355.

Emmons, H.W. & Bryson, A. (1951). The Laminar-Turbulent Transition in a Boundary Layer-Part II, *Proceeding of 1st U.S. Nat. Congress of Theoratical and Applied Mechanics*, pp. 859-868.

Emmons, H W. (1951). The Laminar-Turbulent Transition in Boundary Layert-Part I. *Journal of the Aeronautical Sciences* , Vol. 18, No. 7, pp. 490-498.

Ergin, F.H. & White, B.E. (2006). Unsteady and transitional flows behind roughness elements. *AIAA Journal*, Vol. 44, No. 11, pp. 2504-2514.

Fu, S. & Wang, L. (2008). Modelling the Flow Transition in Supersonic Boundary Layer with a New k-ω-γ Transition/Turbulence Model. *7th International Symposium on Engineering Turbulence Modelling and Measurements-ETMM7*, Limassol, Cyprus, 4-6 June.

Gaster, M. (1967). The structure and behaviour of separation bubbles. *Aeronautical Research Council Reports and Memoranda*, No:3595, London.

Genç, M.S., Lock, G., Kaynak, Ü. (2008). An experimental and computational study of low Re number transitional flows over an aerofoil with leading edge slat, *8. AIAA Aviation Technology, Integration and Operations Conference, ATIO 2008*, Anchorage, Alaska, USA.

Genç, M.S., Kaynak, Ü., Lock, G.D. (2009). Flow over an Aerofoil without and with Leading Edge Slat at a Transitional Reynolds Number, *Proc IMechE, Part G- Journal of Aerospace Engineering*, Vol. 223, pp. 217-231.

Genç, M.S. (2009). Control of Low Reynolds Number Flow over Aerofoils and Investigation of Aerodynamic Performance (in Turkish), PhD Thesis, Graduate School of Natural and Applied Sciences, Erciyes University, Kayseri, TURKEY.

Genç, M.S. (2010). Numerical Simulation of Flow over an Thin Aerofoil at High Re Number using a Transition Model, *Proc IMechE, Part C- Journal of Mechanical Engineering Science*, Vol. 224, pp. 2155-2164.

Genç, M.S., Kaynak, Ü., Yapici, H. (2011). Performance of Transition Model for Predicting Low Re Aerofoil Flows without/with Single and Simultaneous Blowing and Suction, *European Journal of Mechanics B/Fluids*, Vol. 30, pp. 218-235.

Genç, M.S., Karasu, İ., Açıkel, H.H. (2012). An experimental study on aerodynamics of NACA2415 aerofoil at low Re numbers, *Experimental Thermal and Fluid Science*, DOI:10.1016/j.expthermflusci.2012.01.029, in press.

Hain, R., Kähler, C., Radespiel, J. (2009). Dynamics of Laminar Separation Bubbles at Low Reynolds Number Aerofoils. *Journal of Fluid Mechanics*, Vol. 630, pp. 129-153.

Ishii, K., Suzuki, S., Adachi, S. (2003). Effect of Weak Sound on Separated Flow over an Airfoil, *Fluid Dynamics Research*, Vol. 33, pp. 357-371.

Karasu, İ. (2011). Experimental and numerical investigations of transition to turbulence and laminar separation bubble over aerofoil at low Reynolds number flows (In Turkish), MSc. Thesis, Graduate School of Natural and Applied Sciences, Erciyes University, Kayseri, TURKEY.

Katz, J. & Plotkin, A. (1991). Low-Speed Aerodynamics from Wing Theory to Panel Methods, McGraw-Hill, Inc.

Kaynak, Ü. and Gürdamar, E. (2008). Boundary-layer Transition under the Effect of Compressibility for the Correlation Based Model", 46th AIAA Aerospace Sciences Meeting, Reno, NV, AIAA-2008-0774, Jan. 07-10.

King R.M. (2001). Study of an Adaptive Mechanical Turbulator for Control of Laminar Separation Bubbles, Degree of Masters of Science Thesis, Graduate Faculty of North Carolina State University, Aerospace Engineering.

Lang, M., Rist, U., Wagner, S. (2004). Investigations on controlled transition development in a laminar separation bubble by means of LDA and PIV. *Experiments in Fluids*, Vol. 36, pp. 43-52.

Langtry, R. & Menter, F. (2005). Transition Modeling for General CFD Applications in Aeronautics, AIAA Paper 2005-0522.

Langtry, R. & Menter, F. (2006). Overview of industrial transition modelling in CFX. ANSYS technical report TPL 8126.

Lee, H. & Kang S.-H. (2000). Flow characteristics of transitional boundary layers on an airfoil in wakes. *Journal of Fluids Engineering*, Vol. 122, No. 3, pp. 522-532.

Lengani, D., Simoni, D., Ubaldi, M., Zunino, P., Bertini, F. (2011). Turbulent boundary layer separation control and loss evaluation of low profile vortex generators, *Experimental Thermal and Fluid Science*, Vol. 35, No. 8, pp. 1505-1513.

Lian, Y. & Shyy W. (2007). Laminar-Turbulent Transition of a Low Reynolds Number Rigid or Flexible Airfoil. *AIAA Journal*, Vol. 45, No.7, pp. 1501-1513.

Lock, G.D. (2007). Lecture notes: Thermofluids 4-fluid mechanics with historical perspective, University of Bath, UK.

Mayle, R.E. (1991). The Role of Laminar-Turbulent Transition in Gas Turbine Engines. *Journal of Turbomachinery*, Vol. 113, 509-537.

McCullough, G.B. & Gault, D.E. (1951). Examples of Three Representative Types of Airfoil-Section Stall At Low Speed. *NACA Technical Note 2502*, Ames Aeronautical Laboratory Moffet Field, California, USA.

Menter, F.R., Langtry, R.B., Likki, S.R., Suzen, Y.B., Huang, P.G., Völker, S. (2004). A Correlation Based Transition Model Using Local Variables: Part I-Model Formulation. *Proceedings of ASME Turbo Expo 2004*, Vienna, Austria, ASME-GT2004-53452, pp. 57-67.

Menter, F. (1994). Two-equation Eddy Viscosity Turbulence Models for Engineering Applications, *AIAA Journal*, Vol. 32, pp. 1598-1605.

Merzkirch, W. (1974). Flow Visualization. London: Academic Press Inc. Ltd.

Misaka, T. & Obayashi, S. (2006). A Correlation-based Transition Models to Flows around Wings. AIAA Paper 2006-918.

Mohsen, J., (2011). Laminar Separation Bubble: Its Structure, Dynamics and control. Chalmers University Of Technology. Research Report 2011:06.

Mueller, T.J. (1983). Flow Visualization by Direct Injection. *Fluid Mechanics Measurements*, Goldstein, R.J., Ed., Hemisphere, Washington, D.C. pp. 307-375.

Nakano, T., Fujisawa, N., Oguma, Y., Takagi, Y., Lee, S. (2007). Experimental study on flow and noise characteristics of NACA0018 airfoil. *Journal of Wind Engineering and Industrial Aerodynamics*, Vol. 95, pp. 511-531.

Ol, M.V., McAuliffe, B.R., Hanff, E.S., Scholz, U., Kähler, C. (2005). Comparison of Laminar Separation Bubble Measurements on a Low Reynolds Number Airfoil in Three Facilities. *35th AIAA Fluid Dynamics Conference and Exhibit*, 6-9 June, Toronto, Ontario Canada, 5149.

Prandtl, L. (1904). On the motion of a fluid with very small viscosity, *Proceedings of 3rd International Mathematics Congress*, Heidelberg, Vol. 3, pp 484-491.

Ricci, R. & Montelpare, S.A. (2005). Quantative IR Thermographic Method to Study the Laminar Separation Bubble Phenomenon. *International Journal of Thermal Sciences*, Vol. 44, pp. 709-719.

Ricci, R., Montelpare, S.A., Silvi, E. (2007). Study of acoustic disturbances effect on laminar separation bubble by IR thermography. *Experimental Thermal and Fluid Science*, Vol. 31, pp. 349-359.

Rinioie, K. & Takemura, N. (2004). Oscillating Behaviour of Laminar Separation Bubble formed on an Aerofoil near Stall, *The Aeronautical Journal*, Vol. 108, pp. 153-163.

Rizetta, D.P., Visbal, M.R., (2007). Direct numerical simulations of flow past an array of distrubuted roughness elements. *AIAA Journal*, Vol. 45, No. 8, pp. 1967-1975.

Roberts, S.K., Yaras, M.I., (2005). Boundary-Layer Transition Affected by Surface Roughness and Free-Stream Turbulence. *Journal of Fluids Engineering*, Vol. 127, No. 3, pp. 449-457.

Sanders, D.D., O'Brien, W.F., Sondergrad, R., Polanka, M.D., Rabe, D.C. (2011). Prediction Separation and Transitional in Turbine Blades at Low Reynolds Numbers-Part I: Development of Prediction Methodology. *Journal of Turbomachinery*, Vol. 133, pp. 031011/1-031011/9.

Santhanakrishnan, A., Jacob, J.D. (2005). Effect of Regular Surface Perturbations on Flow Over an Airfoil. *35th AIAA Fluid Dynamics Conference and Exhibit*, 6-9 June 2005, Toronto, Ontorio, Canada.

Schlichting, H. (1979). Boundary Layer Theory, McGraw-Hill, Inc, 7th edition.

Schubauer, G.B., Skramstad, H.K. (1947). Laminar boundary layer oscillations and stability of laminar flow. *Journal of Aeronautical Sciences*, Vol. 14, No.2, 69-78.

Selig, M.S., Deters, R. W., Williamson G. A. (2011). Wind Tunnel Testing Airfoils at Low Reynolds Numbers, *49th AIAA Aerospace Sciences Meeting*, 4-7 January, Orlando, FL 875, USA.

Shan, H., Jiang, L., Liu, C., Love, M., Maines, B. (2008). Numerical study of passive and active flow separation control over a NACA0012 airfoil. *Computers & Fluids*, Vol. 37, No. 8, pp. 975-992.

Sharma, M. S. & Poddar, K. (2010). Experimental Investigation of Laminar Separation Bubble for a Flow Past an Airfoil, *Proceedings of ASME Turbo Expo 2010: Power for Land, Sea, and Air (GT2010)*, June 14-18, Glasgow, UK.

Suluksna, K. & Juntasaro, E. (2008). Assessment of Intermittency Transport Equations for Modeling. *International Journal of Heat and Fluid Flow*, Vol. 29, pp. 48-61.

Suzen, Y. B. & Huang, P.G. (2000). Modeling of Flow Transition using an Intermittency Transport Equation. *Journal of Fluids Engineering-Transaction of ASME*, Vol. 122, pp. 273-284.

Suzen, Y. B. & Huang, P.G. (2003). Predictions of Separated and Transitional Boundary Layers under Low-Pressure Turbine Aerofoil Conditions using an Intermittency Transport Equation. *Journal of Turbomachinery*, Vol. 125, pp. 455-464.

Swift, K.M. (2009). An Experimental Analysis of the Laminar Separation Bubble at Low Reynolds Numbers, Msc. Thesis, University of Tennesee Space Institute.

Tan, A.C.N. & Auld, J.D. (1992). Study of Laminar Separation Bubbles at Low Reynolds Number Under Various Conditions. *11th Australasian Fluids Mechanics Conference*, University of Tasmania, Hobart, Australia.

Tani, I. (1964). Low Speed Flows Involving Bubble Separations. *Progress in Aerospace Sciences*, Vol. 5, 70-103.

Torii, K. (1977). Flow Visualization by Smoke-Wire Technique. *Proceedings of the International Symposium on Flow Visualization*, Tokyo, Japan, pp. 251-263.

Uranga, A. (2011). Investigation of transition to turbulence at low Reynolds numbers using Implicit Large Eddy Simulations with a Discontinuous Galerkin method. Ph.D Thesis, Department of Aeronautics and Astronautics, MIT, USA.

University of Washington, Aeronautical Laboratory (UWAL), *http://www.uwal.org/uwalinfo/techguide/flowvis.htm*, access date: January, 2012.

Walters, D.K. & Leylek, J. H. (2004). A New Model for Boundary Layer Transition Using a Single-Point RANS Approach. *Journal of Turbomachinery*, Vol. 126, pp. 193-202.

Walters, D.K. and Leylek, J. H. (2005). Computational fluid dynamics study of wake induced transition on a compressor-like flat plate. *Transactions of the ASME*, Vol. 127, pp. 52-55.

White, F.M. (1991). Viscous fluid flow, Second edition, McGraw-Hill Inc., New York.

White, F.M. (2004). Fluid Mechanics, McGraw-Hill, Inc, 4th edition edition.

Wilcox, D.C. (1994). Simulation of Transition with a Two-equation Turbulence Model. *AIAA Journal*, Vol. 32, pp. 247-255.

Wilcox, D.C. (1998). Turbulence Modeling For CFD, Second Edition, DCW Industries.

Windte J., Scholz, U., Radespiel, R. (2006). Validation of the RANS-simulation of laminar separation bubbles on airfoils. *Aerospace Science and Technology*, Vol. 10, pp. 484-494.

Yang, Z., Haan, L.F., Hui, H. (2007). An Experimental Investigation on the Flow Separation on a Low-Reynolds Number Airfoil. *45th AIAA Aerospace Sciences Meeting and Exhibit*, Reno Nevada.

Yarusevych, S., Kawall, J.G., and Sullivan, P.E. (2007). Separated Shear Layer Transition at Low Reynolds Numbers: Experiments and Stability Analysis, 37th AIAA Fluid Dynamics Conference and Exhibit, 25-28 June, Miami, Florida, USA.

Yarusevych, S., Sullivan, P.E., and Kawall, J.G. (2007). Effect of acoustic excitation amplitude on airfoil boundary layer and wake development. *AIAA Journal*, Vol. 45, No. 4, pp. 760-771.

Yarusevych, S., Sullivan P.E., Kawall, J.G. (2008). Smoke-Wire Flow Visualization on an Airfoil at Low Reynolds Numbers. *38th Fluid Dynamics Conference and Exhibit*, 23-26 June, AIAA-2008-3958, Seattle, Washington, USA.

Yarusevych, S., Kawall, J.G., Sullivan P.E. (2008). Vortex Shedding Characteristics on an Airfoil at Low Reynolds Numbers. *38th Fluid Dynamics Conference and Exhibit*, 23-26 June, AIAA 2008-3957, Seattle, Washington, USA.

Zaman, K.B.M.Q., McKinzie, D.J. (1991). Control of Laminar Separation over Airfoils by Acoustic Excitation. *AIAA Journal*, Vol. 29, pp. 1075-1083.

Zaman K.B. M. Q., (1992). Acoustic Excitation on Stalled Flows over an Airfoil, *AIAA Journal*, Vol. 30, pp. 1492-1498.

Zhang W., Hain R., Kahler C.J. (2008). Scanning PIV Investigation of the Laminar Separation Bubble on a SD7003 Airfoil. *Experiment in Fluids*, Vol. 45, pp. 725-743.

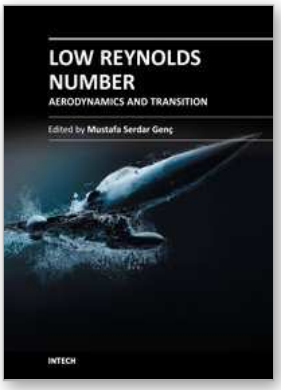

Low Reynolds Number Aerodynamics and Transition

Edited by Dr. Mustafa Serdar Genc

ISBN 978-953-51-0492-6
Hard cover, 162 pages
Publisher InTech
Published online 04, April, 2012
Published in print edition April, 2012

This book reports the latest development and trends in the low Re number aerodynamics, transition from laminar to turbulence, unsteady low Reynolds number flows, experimental studies, numerical transition modelling, control of low Re number flows, and MAV wing aerodynamics. The contributors to each chapter are fluid mechanics and aerodynamics scientists and engineers with strong expertise in their respective fields. As a whole, the studies presented here reveal important new directions toward the realization of applications of MAV and wind turbine blades.

INTECH
open science | open minds

InTech Europe
University Campus STeP Ri
Slavka Krautzeka 83/A
51000 Rijeka, Croatia
Phone: +385 (51) 770 447
Fax: +385 (51) 686 166
www.intechopen.com

InTech China
Unit 405, Office Block, Hotel Equatorial Shanghai
No.65, Yan An Road (West), Shanghai, 200040, China
中国上海市延安西路65号上海国际贵都大饭店办公楼405单元
Phone: +86-21-62489820
Fax: +86-21-62489821